

Carrier Aggregation technique, use of dual-band dish antennas 23GHz/80GHz for 5G requirements

*Note: Work-study project at Orange France

Kweneth KIKHOUNGA

Electronics, Electrical Energy, and Automation Department (EEA)

Faculty of Science and Technology

Montpellier, France

30 Place E. Bataillon, 34095 Montpellier

Abstract—The paper here focuses on the design and optimization of dual-band dish antennas for 5G networks. The primary objective of this project is to meet the 5G requirements by achieving high data rates, optimal coverage, and reliable propagation over distances greater than 5 km. Current engineering solutions typically use single-frequency antennas, on 80 GHz or 23 GHz. However, high-frequency bands, particularly around 80 GHz, are highly sensitive to atmospheric propagation losses, limiting their range and effectiveness.

To address these challenges (improvement of data rates, improvement in coverage and signal quality), we are implementing Carrier Aggregation technique, which combines E-band frequencies with traditional frequency bands (18 GHz or 23 GHz). This approach requires the development of dual-band dish antennas capable of operating simultaneously in two distinct frequency bands while maintaining high performance. The iterative design process with CST Microwave Studio and ATOLL Software aims to optimize the reflection coefficient, gain, and far-field radiation pattern parameters to ensure that antennas meet the stringent technical and reliability requirements of 5G networks. This work contributes to addressing the limitations of current solutions and paves the way for more efficient and scalable 5G deployments.

Index Terms—Dish antennas, dual frequency antenna, gain, signal propagation

I. INTRODUCTION

In the context of 5G deployments, the need for high data rates, optimal coverage, and reliable propagation over distances exceeding 5 km presents significant technical challenges, especially when using high frequencies such as 80 GHz or 23 GHz. These frequencies, while offering high throughput, are sensitive to atmospheric losses, which limit their range and effectiveness. For example, the 80 GHz frequency band, widely used for point-to-point transmissions, suffers from significant propagation losses, reducing its range to less than 5 km. [1]

To overcome these limitations, **Carrier Aggregation technique** has been proposed. This method combines E-band frequencies (80 GHz) with traditional frequency bands (18 GHz or 23 GHz) to improve coverage and reliability. Implementing this solution requires the design of dual-band dish antennas.

Dual-band dish antennas offer considerable advantages with their high directivity, gain exceeding **30 dBi**, and efficiency

93% [2][3]. These antennas enable reliable and efficient transmission over significant distances. Additionally, their optimized design reduces inter-band interference, and minimizes return losses, making them ideal for 5G applications. [4]

In this project, we will use CST Microwave Studio and ATOLL software to design and simulate a dual-band dish antenna. The focus will be on evaluating the following parameters:

- **Radiation pattern and efficiency:** to analyze directional performance.
- **Gain:** to evaluate the efficiency of the antenna in concentrating energy.
- **Reflection coefficients:** to evaluate the impedance match and ensure a low return loss.
- **Coupling coefficient:** to minimize coupling between the two frequency bands (80 and 23 GHz) and prevent interference.

The simulation results will be compared to those of existing antennas to adjust and optimize performance in terms of gain, radiation pattern, and interband isolation. This iterative process will ensure that the antenna meets the strict technical and reliability requirements for the 5G deployment.

II. ANTENNA BASICS

In this part we are going to define some fundamental notions about antennas.

1) **Bandwidth:** The bandwidth of an antenna is defined as the range of frequencies where the reflection coefficient $S_{11} < -10$ dB.

2) **Gain:** The gain of an antenna represents its ability to concentrate electromagnetic radiation toward a specific direction compared to a perfect isotropic antenna ¹. [5]

3) **Antenna Efficiency:** Resistive losses, due to non perfect metals and dielectric materials, exist in all practical antennas. Such losses result in a difference between the power delivered

¹An isotropic antenna is a theoretical antenna that radiates power uniformly in all directions.

to the input of an antenna and the power radiated by that antenna. As with many other electrical components, we can define the efficiency of an antenna as the ratio of the desired output power to the supplied input power. In general, the overall efficiency can be written as [2] :

$$\eta_0 = \eta_r \eta_c \eta_d \quad (1)$$

where:

- η_0 = total efficiency,
- η_r = reflection (mismatch) efficiency,

$$\eta_r = (1 - |S_{11}|^2) \quad (2)$$

- η_c = conduction efficiency,
- η_d = dielectric efficiency.

S_{11} is the reflection coefficient, which determines how much power is reflected instead of being transmitted into the antenna [3].

4) **Polarization:** Polarization of an antenna in a given direction is defined as the polarization of the wave transmitted (radiated) by the antenna. In general, polarization of a radiated wave is defined as the property of an electromagnetic wave describing the time-varying direction and relative magnitude of the electric-field vector. [3]

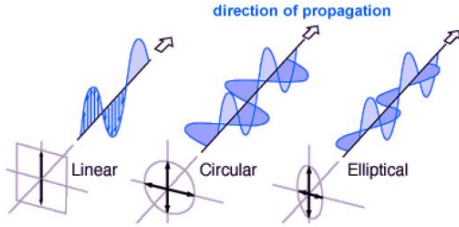


Fig. 1. Antenna polarisation

5) **Radiation pattern:** An antenna radiation pattern or antenna pattern is defined as the representation of the emitted or received power in three dimensions, normalized with respect to the maximum power. Often, two planes are chosen : the horizontal plane or azimuth plane or H-plane (xOy) and the vertical plane or elevation plane or E-plane (yOz). [5]

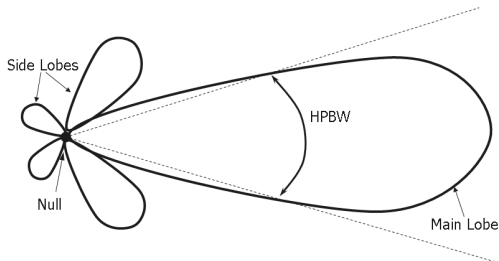


Fig. 2. 2D Directional Antenna-Beam pattern in E-plane

III. ANTENNA DESIGN

Several types of antenna can be used for wireless communication links. In this article, we focus on dual-band dish cassegrain antennas, which play a crucial role in ensuring reliable point-to-point communication, particularly for 5G networks. [2]

A. Parabolic or reflector antenna

The parabolic or reflector antenna, first introduced by Heinrich Hertz in 1888, was designed to focus the radiated field from a focal source by correcting its phase via reflection. [6]

Dish antenna consists in a parabolic reflector associated with a primary feed system, with a waveguide antenna or horn or microstrip.

These antennas are ideal for long-distance communications due to their unique characteristics: **high gain, high efficiency, and wide bandwidth.**

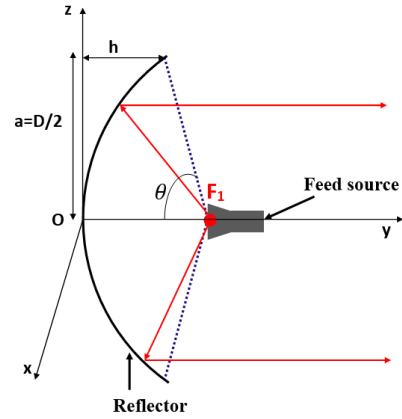


Fig. 3. Schematic of a dish antenna

1) **Materials:** Aluminum, a lossy metal, is often used for the reflector.

2) **Primary Focus (F1):** The ratio of the focal length to the diameter of the reflector is calculated using the following formula:

$$F_1 = \frac{a^2}{4h} \quad (3)$$

where:

- F_1 : Focus (in m),
- a : reflector radius (in m),
- h : height of the reflector (in m).

3) **Opening Angle:** The opening angle, also known as the illumination angle, is the total angle of the cone within the antenna that focuses or captures most of its power. It is given by :

$$\theta = 2 \arctan \left(\frac{D}{4F_1} \right) \quad (4)$$

where:

- θ : opening angle (in deg.),
- D : reflector diameter (in m).

When $\theta < 20$ deg, the antenna is said to be very "directive".

4) **Antenna Gain:** The antenna gain is given by the following formula :

$$G = \eta \left(\frac{\pi D f}{c} \right)^2 \quad (5)$$

where:

- G : Gain (in dBi),
- η : total efficiency of the antenna,
- D : diameter of the parabolic reflector (in m),
- f : frequency (in Hz),
- c : speed of light (in m/s)

B. Cassegrain antenna

This device is named after the 17th-century French physicist and astronomer, Laurent Cassegrain, who improved Newton's telescope to create the double reflector system that bears his name. The system consists of combining a hyperbolic secondary reflector and a parabolic main reflector, as shown in figure 4.

The focal source is placed at the focus, at a sufficient distance from the secondary reflector so that it is considered in the far field. This secondary reflector is sized to limit spillover losses and thus optimize the illumination law [6].

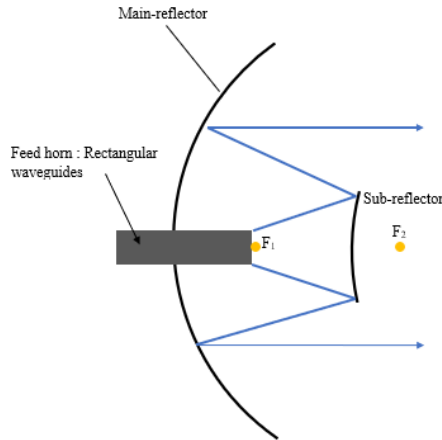


Fig. 4. Cassegrain antenna with feed horn

The advantage of using such a system is mainly to limit phase aberrations. Moreover, the side lobes of its radiation pattern are lower, and the gain drops are less significant compared to a single-reflector parabolic antenna.

1) **Subreflector:** The subreflector is **hyperbolic**, defined by the equation:

$$z = \frac{r^2}{2C} \quad (6)$$

C is the curvature determined by F_2 (the focal point), and r the hyperbolic radial.

2) **Secondary focus F_2 :** It represents the focal points of the hyperbolic sub-reflector. The incident wave which is coming from the feed is firstly reflected by the sub-reflector at the secondary focus and then redirected to the main reflector to be collimated.

IV. TECHNICAL SPECIFICATIONS

As part of this project, we will use two specific frequency bands allocated to Orange:

- The **80 GHz** band, which offers a wide bandwidth but is highly attenuated by the atmosphere.
- The **23 GHz** band, which has a longer range but a lower bandwidth.
- A desired gain of at least **30 dBi** and an antenna efficiency of at least **93%**.

The carrier aggregation technique will allow us to combine these bands to enhance signal quality and reliability. However, to utilize these frequencies simultaneously, it is necessary to design an optimized dual-band antenna.

A. Cassegrain Antenna Design

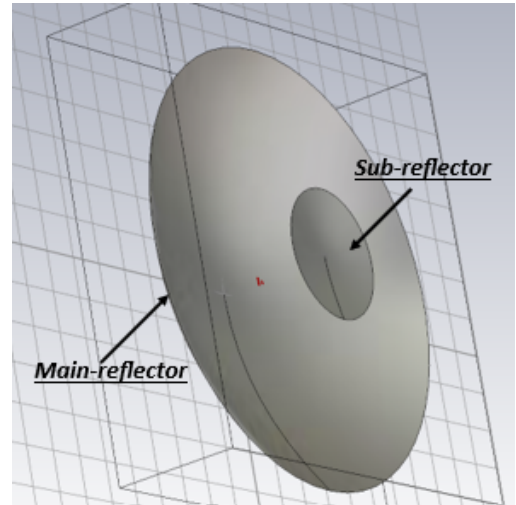


Fig. 5. Structure of a cassegrain antenna, designated on CST

The antenna was designed using CST Studio software, with precise dimensions to ensure optimal propagation of the frequencies specified in the technical specifications.

B. Design of the Antenna Feed System

We will use two standard rectangular waveguides, WR42 (band K) for the 23 GHz and WR12 (band E) for the 80 GHz as feed horn. The two waveguides will be stacked on top of each other. They will be positioned at the (F_1) of the parabolic reflector. The electromagnetic waves emitted from the feed horn are first reflected by the sub-reflector, then redirected towards the main parabolic reflector, and finally all the wave beams reach the aperture of the antenna.

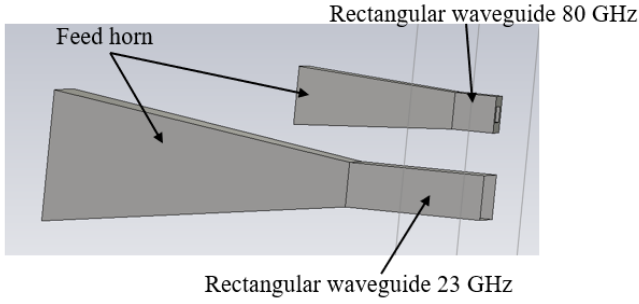


Fig. 6. Side view of waveguides

Here is a summary table of the calculations made; it contains all the parameters necessary for the design of our antenna on CST.

TABLE I
DESIGN PARAMETERS FOR CASSEGRAIN PARABOLIC ANTENNA

Parameters	Values
Main-reflector geometry	
Reflector Diameter (D)	0.558 m
Primary focus (F_1)	0.187 m
Height of main-reflector (h)	0.0126 m
Opening angle $2(\theta_0)$	1.278 deg.
Distance (d)	0.08 m
Antenna Aperture Efficiency (η)	0.70
Sub-Reflector Geometry	
Sub-Reflector Diameter (D_s)	0.164 m
Secondary Focus (F_2)	0.093 m
Rectangular Waveguide WR42	
Length (a)	0.0107 m
Width (b)	0.0043 m
Rectangular Waveguide WR12	
Length (a)	0.0031 m
Width (b)	0.0015 m
Material Properties	
Relative Permeability (μ_r)	1.0
Electrical Conductivity (σ)	3.56×10^7 S/m
Operating frequencies (f)	23/80 GHz

V. SIMULATION AND RESULTS

A. Simulation Tool: CST Studio Suite

CST Studio Suite is an electromagnetic simulation software used to design and analyze electromagnetic components and systems, particularly in high-frequency, microwave domain and optics applications.

In this project, we have chosen the Integral Equation Solver to solve Maxwell's equation. Indeed, The Integral Equation Solver is a 3D full-wave solver, based on the method of moments (MOM) which solves Maxwell's equations using surface currents, reducing the computational domain to the object's surface instead of meshing the entire volume. [7]

Once the two waveguides and caessegrain antenna have been designed, the waveguides will be integrated into the

main-reflector using CST to perform the simulations. Each waveguide will be assigned a port :

- **Port 1** for the **23 GHz waveguide**: Ant_{23}
- **Port 2** for the **80 GHz waveguide**: Ant_{80}

The simulations are run individually; first of all we will simulate the reflection coefficients (S_{11}) at 23 GHz for the Ant_{23} and (S_{22}) at 80 GHz for the Ant_{80} . Then the coupling coefficients (S_{12}) and (S_{21}) between the Ant_{23} and Ant_{80} .

This will help assess the level of interference and coupling between the two frequency bands.

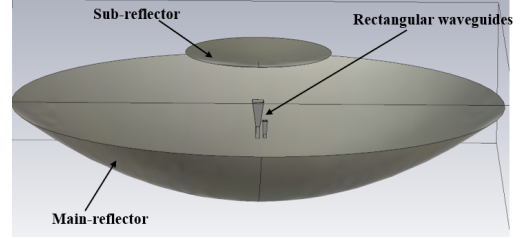


Fig. 7. Final antenna design with integrated source waveguides

B. Results

1) **Reflection coefficient $S(1,1)$ and $S(2,2)$** : I have obtained a reflection coefficient $S(1,1) = -13.49$ dB at 23 GHz and $S(2,2) = -24.32$ dB at 80 GHz, representing the signal reflection at Ant_{23} and Ant_{80} , respectively.

Interpretation of $S(1,1)$:

A value of -13.49 dB indicates that only a small portion of the signal is reflected, while the majority is successfully transmitted into the antenna structure. It is therefore matched.

Some reflection still exists, meaning there could be slight mismatches in the waveguide-feed or the reflection due to the reflectors.

Interpretation of $S(2,2)$:

Now we are analyzing the reflection at 80 GHz for the Ant_{80} . A value of -24.32 dB means that most of the power is transmitted to the structure of the antenna. In practical terms, this means good impedance matching at 80 GHz.

2) **Coupling coefficients**: The Coupling coefficients are represented by S_{12} and S_{21} .

In fact, S_{12} is equivalent to the transmission coefficient from port 2 to port 1. It means that we are applying an incident wave at Ant_{80} and measuring the outgoing wave at Ant_{23} . Similarly, S_{21} represents the transmission coefficient from Port 1 to Port 2, where an incident wave is applied at Ant_{23} , and the outgoing wave is measured at Ant_{80} .

Interpretation of $S(1,2)$:

We have transmitted the signal from Ant_{80} and are now observing its effect at Ant_{23} .

When Ant_{80} is excited at a frequency of 80 GHz, we obtain $S(1,2) = -21.34$ dB, indicating low coupling at this frequency. This suggests some interaction between the

two waveguides. The signal is not completely cut off by the WR42 waveguide Ant_{23} ; this rather corresponds to the excitation of a higher-order mode within the waveguide (WR42), which subsequently couples with the fundamental mode of WR12.(Ant_{80}).

Interpretation of $S(2,1)$:

Here, the signal is transmitted from Ant_{23} and observing its effect at Ant_{80} .

When we excite the Ant_{23} at $f=23$ GHz, $S(2,1) = -57.69$ dB, that means a very low coupling at this frequency which indicates that almost no power from Ant_{23} is transferred to Ant_{80} .

To better understand it, let's calculate the cutoff frequency of the fundamental mode of the WR12 waveguide. For the fundamental mode (TE_{10}), the cutoff frequency is given by:

$$f_c = \frac{c}{2a} \quad (7)$$

where $a = 3.1$ mm. This gives:

$$f_c = 48.38 \text{ GHz} \quad (8)$$

As $f < f_c$, this means that the signal at 23 GHz will not propagate within the WR12 waveguide.

3) Farfield Radiation Pattern (3D), Gain Pattern and Antenna Efficiency: Fig.8 shows the farfield radiation pattern of our cassegrain dish antenna with two waveguides feed one at 23 GHz and the other at 80 GHz.

The radiation pattern of the antenna is very much directive and beamwidth is narrow.

From fig.8 it can be seen that the realized gain of the antenna is about 39.4 dBi and 39.9 dBi, and the radiation efficiencies are 0.00668 dB and 0.003868 dB, respectively at excitation frequencies of 23 GHz and 80 GHz. The antenna efficiencies are 99.55% for 23 GHz and 98.96% for 80 GHz.

This very high antenna efficiency indicates that minimal power is lost due to material losses or impedance mismatches. The antenna is well-optimized for radiation, meaning most of the input power is effectively converted into radiated electromagnetic waves.

Fig.9 shows the 2D farfield gain pattern of the antenna. The main lobe magnitude is -0.621 dB, the main lobe direction is 0 deg and 3 dB angular beamwidth is 0.8 deg. and side lobe level is -24.6 dB for the Ant_{23} . Those informations mean that the antenna is well aligned and the beamwidth is very narrow indicating a highly directive antenna. This narrow beam ensures long-distance, point-point communication with minimal losses.

For the Ant_{80} , the main lobe magnitude is 0 dB, the main lobe direction is 2.0 deg. and 3 dB angular beamwidth is 0.7 deg. and side lobe level is -2.8 dB. Here, the main lobe at 2.0 deg indicates a small misalignment at 80 GHz. The antenna is also directional at 80 GHz focusing all energy.

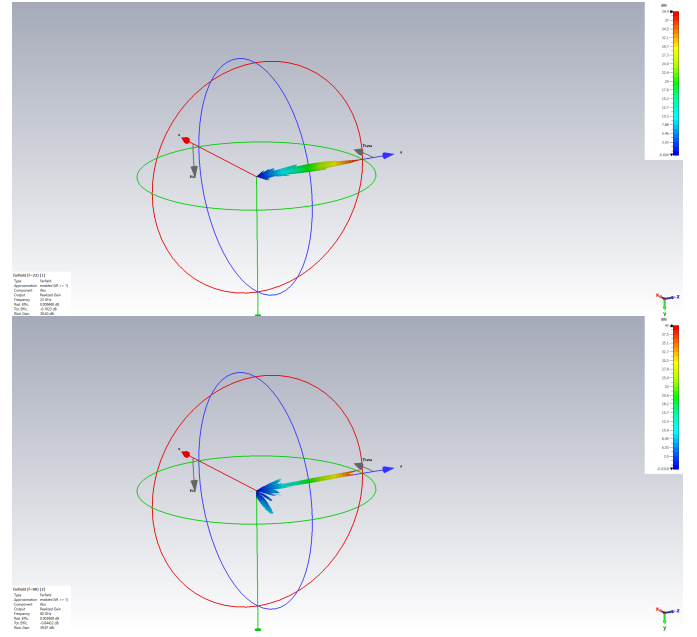


Fig. 8. 3D Farfield radiation pattern

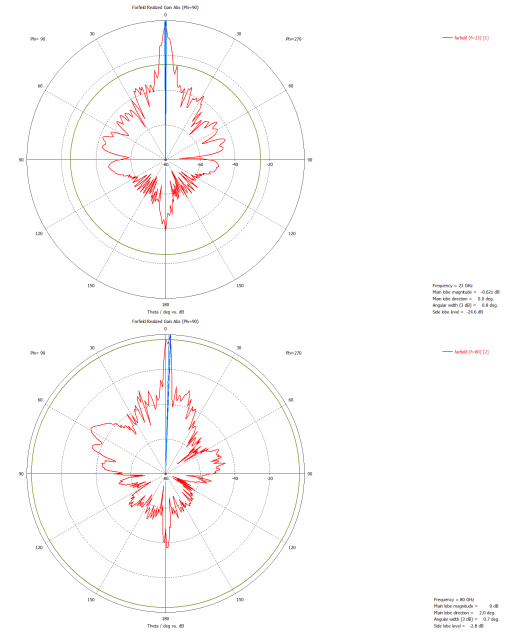


Fig. 9. 2D Farfield gain pattern

return loss, coupling parameters, farfield radiation pattern, antenna gain and antenna efficiency of the proposed antenna system show reasonable characteristics. The performance of the antenna is good. This antenna can be used in both E-band and K-band applications for its effective performance.

TABLE II
OVERALL SIMULATION RESULTS FOR CASSEGRAIN ANTENNA

Antenna Parameters	Simulation Results	
	<i>Ant</i> ₂₃	<i>Ant</i> ₈₀
Reflection Coef. (in dB)	- 13.49	- 24.33
Coupling Coef. (in dB)	- 21.34	- 57.69
Gain (<i>dBi</i>)	39.4	39.9
Half Power Beamwidth	0.8 deg.	0.7 deg.
Antenna Efficiency (%)	99.55	98.96

VI. CONCLUSION

This project focused on the design, simulation, and analysis of a **dual-band Cassegrain dish antenna** operating at **23 GHz and 80 GHz** for **5G backhaul applications**. The primary objective was to implement **Carrier Aggregation** to improve signal reliability and data rates by combining **E-band (80 GHz)** with lower frequency bands (**23 GHz**).

Through extensive simulations conducted using CST Studio Suite, the antenna's performance metrics, including reflection coefficients ($S(1,1)$, $S(2,2)$), coupling coefficients ($S(2,1)$, $S(1,2)$), radiation patterns, and gain, were evaluated to ensure optimal efficiency. The results demonstrated that :

- The **reflection coefficients** confirm **good impedance matching** at both frequencies, with $S(1,1) = -13.49$ dB at **23 GHz** and $S(2,2) = -24.33$ dB at **80 GHz**.
- The **coupling coefficients** show **low inter-band interference**, with $S(1,2) = -23.64$ dB and $S(2,1) = -57.59$ dB, confirming **minimal signal leakage** between the two frequency bands.
- The **far-field radiation patterns** reveal **highly directive beams**, with **beamwidths of 0.8° at 23 GHz and 0.7° at 80 GHz**, ensuring focused signal transmission.
- The **realized gains of 39.4 dBi at 23 GHz and 39.9 dBi at 80 GHz** validate the antenna's high directivity and efficiency.
- The **antenna efficiency of 99.55% at 23 GHz and 98.96% at 80 GHz** confirms minimal power losses, making the design highly efficient.

These results demonstrate that the proposed **dual-band Cassegrain antenna** is well-suited for long-distance, high-data-rate communication, providing strong coverage and high reliability in 5G networks.

FUTURE WORK AND OPTIMIZATIONS

In the future, we should work on waveguides. Find a better solution for superimposing the two guides to minimise adaptation losses at high frequencies. Characterise each waveguide individually and the two assemblies without the dish and with the dish. Position the waveguides correctly to limit coupling between the two frequencies.

ACKNOWLEDGMENT

I would like to express my gratitude to Sylvie JARRIX, Professor at the University of Montpellier, my academic supervisor, for reviewing and correcting this report. I also sincerely

thank Professor Annick PENARIER, for providing me with access to the CST Studio simulation tool and for her guidance throughout the simulation process. Finally, I would like to extend my appreciation to Ms. Aline LENOIR, my company supervisor, and Ms. Sophie GABOYARD, my manager, for their support and valuable mentorship.

REFERENCES

- [1] Alcatel. (2002). Publication. Connaissance des liaisons hertziennes. Orange France
- [2] Balanis, C. A. (2016). Antenna Theory: Analysis and Design. John Wiley Sons.
- [3] Pozar, David M. (2005); Microwave Engineering, Third Edition (Intl. Ed.); John Wiley Sons, Inc.; pp. 170-174. ISBN 0-471-44878-8.
- [4] Balanis, C. A. (2016). Antenna Theory: Analysis and Design. John Wiley Sons. pp. 70
- [5] Cours de base des antennes, Sylvie JARRIX, Université de Montpellier.
- [6] Wassim Saleh. Étude de nouvelles technologies d'antennes pour applications 5G dans la bande millimétrique.. Electronique. UNIVERSITE DE NANTES, 2021. Français. NNT : .tel-03430428.
- [7] Dassault Systèmes, CST Studio Suite 2024 - Integral Equation Solver User Guide.
- [8] IEEE Transactions on Antennas and Propagation, Vols. AP-17, No. 3, May 1969; Vol. AP-22, No. 1, January 1974; and Vol. AP-31, No. 6, Part II, November 1983
- [9] Cyrille MENUDIER. Thèse: Caractérisation des performances d'antennes à réflecteurs paraboliques illuminées par une source focale BIE. Application à l'optimisation d'une couverture multimédia multi-faisceaux, 2007, UNIVERSITE DE LIMOGES
- [10] J. Clerk Maxwell, A Treatise on Étude de nouvelles technologies d'antennes pour applications 5G dans la bande millimétrique, 3rd ed., vol. 2. Oxford: Clarendon, 1892, pp.68–73.
- [11] Anindya Kumar Kundu, MD. Tofael Hossain Khan, "Design and Performance Analysis of a Dual Band Parabolic Reflector Antenna with Waveguide Dipole Feed and Link Budget Optimization," in proceedings of the 2nd International Conference on Advances in Electrical Engineering (ICAEE 2013) 19-21 December 2013, Dhaka, Bangladesh
- [12] Padmasree Ramineni, "Design and Analysis of a Dual-Band Microstrip Patch Antenna for Sub-6 GHz Applications," Ramineni; J. Eng. Res. Rep., vol. 26, no. 7, pp. 210-221, 2024; Article no.JERR.118394.